Available online at www.sciencedirect.com

ScienceDirect

Inorganica Chimica Acta 361 (2008) 1298–1310

Inorganica Chimica Acta

www.elsevier.com/locate/ica

Silver coordination complexes of 2-(diphenylphosphinomethyl) pyridine and their bipyridine derivatives

Fernando Hung-Low, Kevin K. Klausmeyer *

Department of Chemistry and Biochemistry, Baylor University, Waco, TX 76798, United States

Received 13 July 2007; accepted 18 August 2007
Available online 25 August 2007

Abstract

Reaction of 2-(diphenylphosphinomethyl)pyridine (PMP-21) with the silver(I) salts of tetrafluoroborate (BF_4^-), triflate (Otf^-), and trifluoroacetate (tfa^-) affords dinuclear complexes (**2**–**4**), where the ligand bridges the two silver centers, and the anions interact with the metal centers to varying degrees. Further reaction of $AgBF_4$ and AgOtf with reaction solutions containing PMP-21 and either the bidentate 5,5′-dimethyl-2,2′-bipyridine or 4,4′-bipyridine ligands produce dimeric and bridged structural motifs. The ability of 5,5′-dimethyl-2,2′-bipyridine to chelate and the 4,4′-bipyridine to serve as a connector between metal centers, allows the construction of coordinative structures where the effect of ligand ratio and either interacting or non interacting anions influence the silver coordination environment, allowing it to take on several geometries including trigonal bipyramidal, **5**, both T-shaped and tetrahedral in a single structure, **6** and **8**, trigonal pyramidal, **7**, and trigonal planar, **9**. Structures **2**, **3**, and **4** display comparable Ag–Ag contacts ranging from 2.7979(10) to 3.0538(4) Å, with a corresponding weakening of the metallophilic interaction when a bipyridine ligand is coordinated. Low-temperature luminescence spectra were collected for all compounds and are compared.

Keywords: N,P ligands; Metal–metal interaction; Silver; Coordination modes

1. Introduction

The coordination behavior of phosphine ligands which also contain a pyridine moiety has been studied for many years [1–3]. The incorporation of harder pyridyl substituents in conjunction with a softer phosphorus center alters and augments the coordination flexibility of the ligand and leads to multidentate hemilabile ligands [4,5]. Free rotation about the P–C_{ipso} bond of pyridyl and 2-methylpyridyl derivatives allows the nitrogen to obtain the correct orientation to coordinate metals of different radii, and in addition to the geometrical flexibility, they provide electronic adaptability as well [6,7]. The multidentate 2-(phosphinomethyl) pyridines of the type $PPh_x(CH_2py_{3-x})$($x = 0$, 1, 2) are potentially interesting ligands in this respect. Of particular interest to this study is the ambidentate ligand 2-(diphenylphosphinomethyl)pyridine (PMP-21, Fig. 1), which can act in a chelating fashion for metal centers that easily adopt L–M–L angles of 90° [8,9]. With metals that do not easily adopt an octahedral environment such as silver(I) it was anticipated that the ligand would act as a bridge suitable for the formation of dinuclear complexes in which the metal ions are held in close proximity, thus allowing direct metal–metal interactions.

The study of d^{10} "closed-shell" interactions that exist between the monovalent elements of group 11 has been active for many years [10–12]. These interactions are typically associated with ligand-bridged, hydrogen-bonded, electrostatically-attracted, or π–π stacked effects, though unsupported M–M interactions have been described as well [13–18]. With silver in particular, crystal engineering of coordination architectures has emerged as a promising field of investigation for the design and construction of novel discrete and polymeric metal–organic coordination

---

* Corresponding author. Fax: +1 254 710 4272.
E-mail address: Kevin_Klausmeyer@baylor.edu (K.K. Klausmeyer).

0020-1693/$ - see front matter © 2007 Elsevier B.V. All rights reserved.
doi:10.1016/j.ica.2007.08.015

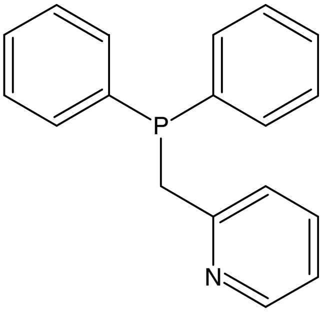

Fig. 1. Structure of PMP-21 ligand.

complexes, with potential use as functional materials [19–23]. The many silver coordination architectures reported are demonstrative of the influence that slight variations in ligand and/or anion imparts on the formation of unique and discrete molecules, supramolecular arrays, and 1-, 2-, and 3-dimensional coordination networks [15–18,24–30]. To date, several reports of the PMP-21 ligand coordinated to transition metals such as Rh [9], Fe, and Ru [31–33] with potential application in the catalysis arena have been published [34], but no systematic investigation of the interaction between this P,N-donor and silver salts has been reported. In this report, we fill the void by the synthesis and spectroscopic characterization of a number of AgX:PMP-21 complexes supported by single-crystal X-ray studies.

Additionally the use of bipyridine ligands (5,5′-dimethyl-2,2′-bipyridine and 4,4′-bipyridine) in the coordination chemistry associated with the AgX:PMP-21 adducts for the formation of mixed ligand coordination complexes is reported. The complexes described in this paper were obtained by varying the ligand/metal ratio and by changing the counterion of the system. Herein, we describe the changes that are brought about in the flexible coordination sphere of the silver(I) cation by the coordination of the bipyridine ligand to the corresponding AgX:PMP-21 complex, and the luminescence that results from the different Ag–P interactions encountered in each metal compound. The PMP–*nm* naming convention that we have adopted allows for ease in discussion of these phosphinomethylpyridines, as there are many substitutions that can be made and systematic nomenclature can be cumbersome. As such, PMP indicates the PhosphinoMethylPyridine ligands, where *n* is the position of substitution on the pyridyl ring and *m* is the number of substitutions by methylpyridine on the phosphorus.

2. Experimental

2.1. General remarks

All experiments were carried out under a nitrogen atmosphere using a Schlenk line and standard Schlenk techniques. All silver salts reagents were stored in an inert-atmosphere glovebox; solvents were distilled under nitrogen from the appropriate drying agent immediately before use. *n*-Butyllithium and chlorodiphenylphosphine were purchased from Aldrich and used as received. Silver(I) trifluoroacetate, silver(I) trifluoromethanesulfonate, and silver(I) tetrafluoroborate were purchased from Strem Chemicals Inc. and used as received. ^{1}H were recorded at 360.13 MHz with a Bruker Spectrospin 300 MHz spectrometer and ^{31}P and variable-temperature ^{31}P NMR spectra were recorded at 202.31 MHz on a Varian 500 MHz NMR spectrometer. Elemental analyses were performed by Atlantic Microlabs Inc. in Norcross, Georgia. Excitation and emission spectra were recorded with an Instruments S.A. Inc. Fluoromax-2 model spectrometer using band pathways of 5 nm for both excitation and emission and are presented uncorrected.

2.2. Synthesis

2.2.1. Synthesis of 2-(diphenylphosphinomethyl)pyridine, PMP-21 (1)

n-Butyllithium (17 mmol, 5.86 mL, 2.9 M in hexane) was added over a period of 10 min to 2-picoline (17 mmol, 1.67 mL) in dry THF (20 mL) at −41 °C. After stirring for 1 h, the mixture was added to a solution of chlorodiphenylphosphine (3.0 g, 17 mmol) in dry THF (20 mL) at −84 °C over a period of 30 min. Water (20 mL) was then added over 10 min and the mixture stirred for 30 min. The product was obtained by first extracting with 0.3 N HCl (aq.), then neutralizing with a $NaHCO_3$ solution, and extracting with dichloromethane. The solvent and any un-reacted 2-picoline were removed under vacuum (oil pump) and a yellow oil resulted. The yield of the crude product was 81%. Purification of the ligand was carried out by several extractions with dry hexane. After removing the solvent a white solid of >98% purity in 70% yield was obtained. ^{31}P NMR ($CDCl_3$, 298 K) δ: (s, −13.73).

2.2.2. Synthesis of $[AgBF_4(PMP\text{-}21)]_2$ (**2**)

To a stirred solution of $AgBF_4$ (0.077 g, 0.396 mmol) in CH_3CN (5 mL) was added **1** (0.109 g, 0.396 mmol) in CH_3CN (5 mL). The resulting solution was allowed to stir for 5 min and then dried in vacuo to leave an off-white powder. This was then dissolved in a small amount of CH_2Cl_2 and precipitated with hexane. The recrystallization was repeated until compound **2** was obtained as a white powder upon drying in 63% (0.117 g, 0.124 mmol) yield. Colorless blocks were obtained by slow diffusion of hexane into a CH_2Cl_2 solution of **2** at 5 °C. ^{1}H NMR ($CDCl_3$, 298 K) δ: 4.05 (m, 4H), 6.65 (d, 2H), 7.48 (m, 8H), 7.60 (m, 16H), 8.89 (d, 2H). ^{31}P NMR ($(CD_3)_2CO$, 238 K) δ: 14.8, dd, $J(^{107}Ag\text{–}P) = 715$ Hz, $J(^{109}Ag\text{–}P) = 629$ Hz, $C_{36}H_{32}Ag_2B_2F_8N_2P_2$ (943.94): *Anal.* Calc. C, 45.81; H, 3.42; N, 2.97. Found: C, 46.04; H, 3.53; N, 3.19%.

2.2.3. Synthesis of $[AgOtf(PMP\text{-}21)]_2$ (**3**)

To a stirred solution of AgOtf (0.109 g, 0.399 mmol) in CH_3CN (5 mL) was added **1** (0.109 g, 0.399 mmol) in

CH_3CN (5 mL). The resulting solution was allowed to stir for 5 min and then dried in vacuo to leave an off-white powder. The compound was re-crystallized with CH_3CN/ether solutions upon drying in 71% (0.151 g, 0.141 mmol) yield. Colorless blocks were obtained by slow diffusion of hexane into a CH_2Cl_2 solution of **3** at 5 °C. ^1H NMR ($CDCl_3$, 298 K) δ: 4.36 (s, 4H), 7.08 (d, 2H), 7.54 (m, 10H), 7.61 (m, 4H), 7.81 (m, 10H), 8.92 (d, 2H). ^{31}P NMR ($(CD_3)_2CO$, 238 K) δ: 13.17, dd, $J(^{107}Ag–P) = 725$ Hz, $J(^{109}Ag–P) = 628$ Hz, $C_{38}H_{32}Ag_2F_6N_2O_6P_2S_2$ (1068.46): *Anal.* Calc. C, 42.72; H, 3.02; N, 2.62. Found: C, 42.77; H, 3.16; N, 2.55%.

2.2.4. Synthesis of [Agtfa(PMP-21)]$_2$ (4)

This reaction used **1** (0.109 g, 0.398 mmol) in CH_3CN (5 mL) added to a stirred solution of Agtfa (0.880 g, 0.398 mmol) in CH_3CN (5 mL) to leave a fluffy off-white solid upon evaporation of the solvent. The compound was purified by washing with CH_2Cl_2 since it is insoluble in the solvent. Upon drying the compound, the product was obtained in 82% (0.325 g, 0.163 mmol) yield. Colorless blocks were obtained by slow diffusion of hexane into a CH_2Cl_2 solution of **4** at 5 °C. ^1H NMR ($CDCl_3$, 298 K) δ: 4.04 (d, 4H), 6.87 (d, 2H), 7.37 (m, 2H), 7.47 (m, 8H), 7.57 (m, 4H), 7.70 (m, 10H), 8.69 (d, 2H). ^{31}P NMR ($(CD_3)_2CO$, 238 K) δ: 11.5, dd, $J(^{107}Ag–P) = 700$ Hz, $J(^{109}Ag–P) = 608$ Hz, $C_{83}H_{70}Ag_4Cl_6F_{12}N_4O_8P_4$ (2247.49): *Anal.* Calc. C, 48.22; H, 3.24; N, 2.81. Found: C, 48.09; H, 3.25; N, 2.83%.

2.2.5. Synthesis of [AgBF$_4$(PMP-21)(5,5′-dimethyl-2,2′-bipyridine)]$_2$ (5)

To a stirred solution of AgOtf (0.109 g, 0.399 mmol) was added 1 equiv. of 5,5′-dimethyl-2,2′-bipyridine (0.074 g, 0.401 mmol) in CH_3CN (5 mL). This was stirred for 5 min, and then a solution of **1** (0.109 g, 0.398 mmol) in CH_3CN (5 mL) was added to the reaction mixture. The solution was stirred for 10 min, and then the solvent was removed in vacuo to leave a light yellow powder in 65% isolated yield (0.170 g, 0.129 mmol). Crystallization formed colorless blocks obtained by slow diffusion of hexane into a CH_2Cl_2 solution of **5** at 5 °C. ^1H NMR ($CDCl_3$, 298 K) δ: 2.41 (s, 12H), 4.51 (d, 4H), 7.31 (m, 2H), 7.51 (m, 2H), 7.63 (m, 11H), 7.99 (m, 14H), 8.25 (d, 7H), 8.46 (s, 2H) 8.70 (m, 2H). ^{31}P NMR ($(CD_3)_2CO$, 238 K) δ: 12.4, br. s, $C_{62}H_{60}Ag_2B_2Cl_4F_8N_6P_2$ (1482.26): *Anal.* Calc. C, 50.24; H, 4.08; N, 5.97. Found: C, 50.65; H, 4.17; N, 6.55%.

2.2.6. Synthesis of [AgBF$_4$(PMP-21)]$_4$(4,4′-bipyridine) (6)

This reaction used 1 equiv. of $AgBF_4$ (0.077 g, 0.396 mmol) in CH_3CN (5 mL) added to 1 equiv. of **1** (0.109 g, 0.398 mmol) in CH_3CN (5 mL). After stirring for 5 min, a solution of 4,4′-bipyridine (0.031 g, 0.198 mmol) in CH_3CN (5 mL) was added, and the mixture was then stirred for 10 min. Upon evaporation of the solvent, a light yellow powder was isolated in 71% yield (0.292 g, 140 mmol). Crystallization formed colorless blocks obtained by slow diffusion of hexane into a THF solution of **6** at 5 °C. ^1H NMR ($CDCl_3$, 298 K) δ: 4.51 (s, 8H), 7.22 (m, 4H), 7.50 (m, 31H), 7.82 (m, 21H), 8.28 (m, 4H), 8.91 (m, 4H). ^{31}P NMR ($(CD_3)_2CO$, 238 K) δ: 14.3, dd, $J(^{107}Ag–P) = 719$ Hz, $J(^{109}Ag–P) = 623$ Hz, $C_{93}H_{88}Ag_4B_4F_{16}N_6O_3P_4$ (2240.29): *Anal.* Calc. C, 45.04; H, 3.16; N, 3.66. Found: C, 44.55; H, 3.49; N, 3.07%.

2.2.7. Synthesis of (AgOtf)$_2$(PMP-21)(5,5′-dimethyl-2,2′-bipyridine)$_2$ (7)

To a stirred solution of AgOtf (0.217 g, 0.798 mmol) in CH_3CN (5 mL) was added a solution of 5,5′-dimethyl-2,2′-bipyridine (0.147 g, 0.798 mmol) in CH_3CN (5 mL). The resulting solution remained clear and colorless, and after stirring for 5 min a solution of 1/2 equiv. of **1** (0.109 g, 0.398 mmol) in CH_3CN (5 mL) was added to the mixture. Upon drying, a light yellow powder in 63% isolated yield (0.304 g, 0.125 mmol) was reclaimed. Colorless blocks crystals were obtained by slow diffusion of hexane into a CH_2Cl_2 solution of **4** at 5 °C. ^1H NMR ($CDCl_3$, 298 K) δ: 2.38 (s, 12H), 4,67 (m, 2H), 7.23 (m, 1H), 7.69 (m, 7H), 7.97 (m, 9H), 8.18 (m, 8H), 9.03 (m, 1H). ^{31}P NMR ($(CD_3)_2CO$, 238 K) δ: 16.5, br. s. $C_{90}H_{85}Ag_4Cl_4F_{12}N_{10}O_{13}P_2S_4$ (2506.14): *Anal.* Calc. C, 44.31; H, 3.26; N, 5.04. Found: C, 43.82; H, 3.33; N, 4.84%.

2.2.8. Synthesis of [AgOtf(PMP-21)]$_4$(4,4′-bipyridine) (8)

To a stirred solution of 2 equiv. of AgOtf (0.217 g, 0.798 mmol) in CH_3CN (5 mL) was added 2 equiv. of **1** (0.221 g, 0.798 mmol) in $5CH_3CN$ (5 mL). This was stirred for 5 min, and then a solution of 4,4′-bipyridine (0.031 g, 0.199 mmol) in CH_3CN (5 mL) was added. This mixture was stirred for 10 min, and then the solvent was removed in vacuo to leave a light yellow powder in 63% isolated yield (0.296 g, 0.125 mmol). Colorless block crystals were obtained by slow diffusion of hexane into a solution of **8** in CH_2Cl_2 at 5 °C. ^1H NMR ($CDCl_3$, 298 K) δ: 4.35 (s, 8H), 7.15 (m, 4H), 7.53 (m, 30H), 7.63 (m, 8H), 7.82 (m, 18H), 8.81 (m, 4H). ^{31}P NMR ($(CD_3)_2CO$, 238 K) δ: 13.0, dd, $J(^{107}Ag–P) = 714$ Hz, $J(^{109}Ag–P) = 631$ Hz, $C_{102}H_{104}Ag_4F_{12}N_6O_{16}P_4S_4$(2581.51): *Anal.* Calc. C, 45.04; H, 3.16; N, 3.66. Found: C, 44.43; H, 3.31; N, 2.99%.

2.2.9. Synthesis of [AgOtf(PMP-21)$_2$]$_2$(4,4′-bipyridine) (9)

To a stirred solution of 2 equiv. of AgOtf (0.217 g, 0.798 mmol) in CH_3CN (5 mL) was added 4 equiv. of **1** (0.442 g, 1.596 mmol) in CH_3CN (5 mL). This was stirred for 5 min, and then a solution of 4,4′-bipyridine (0.062 g, 0.399 mmol) in CH_3CN (5 mL) was added. Upon drying, a light yellow powder in 70% isolated yield (0.496 g, 0.279 mmol) was obtained. Crystallization formed colorless blocks of obtained by slow diffusion of hexane into a solution of **9** in CH_2Cl_2 at 5 °C. ^1H NMR ($CDCl_3$, 298 K) δ: 4.32 (s, 8H), 7.16 (m, 4H), 7.54 (m, 30H), 7.63 (m, 8H), 7.86 (m, 18H), 8.82 (m, 4H). ^{31}P NMR ($(CD_3)_2CO$, 238 K) δ: 12.5, dd, $J(^{107}Ag–P) = 718$ Hz, $J(^{109}Ag–P) = 631$ Hz, $C_{84}H_{72}Ag_2F_6N_6O_6P_4S_2$ (1779.22): *Anal.* Calc. C, 56.58; H, 4.30; N, 4.71. Found: C, 56.05; H, 4.03; N, 5.00%.

3. Results and discussion

3.1. General characterizations

3.1.1. Synthesis and NMR spectra

The ligand 2-(diphenylphosphinomethyl)pyridine (PMP-21) **1**, synthesized by a modified procedure [9], has been effectively purified with several hexane extractions, producing a white powder with >98% purity in 70% yield, as opposed to the creamy colored oil with purity >90% previously reported. Pure **1** is thermally stable and is not found to be readily oxidized in comparison to the less pure creamy yellow oil. The reaction of three different silver(I) salts (BF_4^-, Otf^-, or tfa^-) with an equimolar quantity of **1** gave rise to the compounds [AgX:PMP-21]$_2$ (1:1) (X = BF_4^-, Otf^-, or tfa^-) **2**–**4**. Under the same conditions, reaction of an equivalent of 5,5′-dimethyl-2,2′-bipyridine and 1/2 equiv. of 4,4′-bipyridine in a reaction mixture containing $AgBF_4$ and PMP-21 yield compounds **5** and **6**, respectively. Reaction of two equivalents of the 5,5′-dimethyl-2,2′-bipyridine ligand with a reaction mixture of 2 equiv. AgOtf and 1 equiv. PMP-21 directs the formation of compound **7**. Controlling the PMP-21/Ag ratio in the reaction involving 4,4′-bipyridine, allows the formation of compounds **8** and **9**. No further reaction of the [Agtfa(PMP-21)]$_2$ complex with any of the bipyridine ligands was observed, likely due to the electronically and sterically crowded silver centers of **4**. Altering the reaction sequence to add the bipy first to the Ag salt and with subsequent addition of the PMP-21 ligand yielded only compound **4** upon crystallization.

Solutions of the silver compounds **2**–**4** readily decompose to leave metallic silver and unidentified black byproduct. A light brown color appears almost immediately upon mixing and is indicative of the reaction of **1** with the various silver salts. However, the powders of each complex have proven themselves to be quite robust, withstanding long exposure to air and room temperatures with little sign of decomposition, provided they are shielded from light. Compounds **5**–**8** were isolated from the respective reaction mixture by immediate precipitation of the corresponding white product with ether once the bipyridine ligand is reacted with the AgX and PMP-21 solution. Compound **9** was purified with simple dichloromethane washings of the remaining solid, since the resulting product was insoluble in the solvent.

The ^{1}H NMR spectra of compounds **2**–**9** are, as expected, generally similar. The ^{31}P NMR spectra at −40 °C were recorded in deuterated acetone for all compounds. At this temperature the dissociation of the Ag–P bond is slowed to a time scale where a doublet of doublets signal, due to the two isotopes of Ag, is observed for all compounds except **5** and **7**. The lack of observed coupling for complexes **5** and **7** is likely due to the presence of the strongly binding 5,5′-dimethyl-2,2′-bipyridine which saturates the metal center in solution and only allows significant binding of the phosphorus moiety upon crystallization or precipitation. Chemical shifts and coupling constants are provided in the experimental section.

3.2. Description of the crystal structures

Crystallographic data were collected on crystals with dimensions 0.094 × 0.062 × 0.055 mm for **2**, 0.303 × 0.247 × 0.161 mm for **3**, 0.281 × 0.201 × 0.188 mm for **4**, 0.209 × 0.153 × 0.102 mm for **5**, 0.334 × 0.181 × 0.156 mm for **6**, 0.268 × 0.158 × 0.094 for **7**, 0.320 × 0.160 × 0.100 for **8**, and 0.296 × 0.287 × 0.176 for **9**. Data were collected at 110 K on a Bruker X8 Apex using Mo Kα radiation ($\lambda = 0.71073$ Å). All structures were solved by direct methods after correction of the data using SADABS. Crystallographic data and refinement details for the complexes mentioned herein are found in Tables 1 and 2. The molecular structure of the compounds is displayed in Figs. 2–9. Summary of selected bond lengths, angles, and interatomic distances are given in Tables 3–5. All data were processed using the Bruker AXS SHELXTL software, version 6.10. Hydrogen atoms were placed in calculated positions and all non-hydrogen atoms were refined anisotropically except for the disordered solvent molecules and anions of compound **8**.

3.2.1. Crystal and molecular structure of compounds 2, 3, and 4

The crystal structure of complex **2** is shown in Fig. 2 and is demonstrative of the bridging effect that the PMP-21 ligand displays, forming a 6-membered ring fragment with two interconnecting silver ions. The silver coordination environments that are seen in structures **2**–**4** do not differ greatly from one structure to the next, demonstrating coordination independence of the counterion present (Scheme 1). As shown in Figs. 2–4 the metal centers in **2** exhibit a T-shape geometry and in **3** and **4** capped T-shaped environments since interaction with the respective counterion is encountered, the exception being one of the silver atoms in compound **4**, where the tfa^- counterion has only a weakly interacting Ag1–O(4) distance of 2.661(3) Å. In **2**, although the BF_4^- ions are displayed as non coordinative, the Ag1–F2 and Ag2–F8 distances of 2.692(2) Å and 2.693(3) Å, respectively, suggest a weak interaction. All three complexes display M–M distances in the typical range values for Ag–Ag interactions, varying from 2.7979(10) to 3.0538(4) Å. The bifunctional phosphine ligand bridges the Ag–Ag axis, acting as a bridging bidentate allowing the metals to come close to one another. A repetitive structural feature in common is that the two PMP-21 ligands coordinate head-to-tail, P–Ag–N across the Ag–Ag axis, rather than head-to-head.

Compounds **3** and **4** both display a 1:1 ratio of PMP-21 ligand to metal with only small variances between the two likely arising from the difference in basicity of Otf^- versus tfa^-. According to Table 3, the Ag–P and Ag–N distances

Table 1
Crystallographic data for compounds **2**–**5**

	2	**3**	**4**	**5**
Empirical formula	$C_{36}H_{32}Ag_2B_2F_8N_2P_2$	$C_{38}H_{32}Ag_2F_6N_2O_6P_2S_2$	$C_{83}H_{70}Ag_4Cl_6F_{12}N_4O_8P_4$	$C_{62}H_{60}Ag_2B_2Cl_4F_8N_6P_2$
Formula mass	943.94	1068.46	2247.49	1482.26
a (Å)	12.0138(14)	9.046(3)	19.2216(19)	11.284(2)
b (Å)	22.4294(18)	10.393(3)	11.6882(14)	20.890(4)
c (Å)	13.6037(14)	10.612(3)	19.809(3)	14.498(3)
α (°)	90	86.744(16)	90	90
β (°)	97.885(3)	87.096(16)	102.160(3)	112.210(4)
γ (°)	90	80.804(16)	90	90
V (Å^3)	3631.0(6)	982.4(5)	4350.5(9)	3164.1(9)
Z	4	1	2	2
Crystal system	Monoclinic	Triclinic	Monoclinic	Monoclinic
Space group	$P2_1/n$	$P\bar{1}$	$P2_1/n$	$P2_1/c$
T (K)	110(2)	110(2)	110(2)	110(2)
D_{calc} (g cm^{-3})	1.727	1.806	1.716	1.556
μ (mm^{-1})	1.238	1.263	1.228	0.907
$2\theta_{max}$ (°)	27.63	25.68	26.28	33.18
Reflections measured	28310	13967	41440	26111
Reflections used (R_{int})	8408 (0.0596)	3637 (0.0525)	8624 (0.0483)	10882 (0.0350)
Restraints/parameters	0/469	0/262	0/556	0/390
R_1 [$I > 2\sigma(I)$]	0.0415	0.0479	0.0335	0.0376
wR_2 [$I > 2\sigma(I)$]	0.0712	0.1219	0.0763	0.0849
$R(F_o^2)$ (all data)	0.0690	0.0544	0.0465	0.0520
$R_w(F_o^2)$ (all data)	0.0812	0.1270	0.0836	0.0942
Goodness-of-fit on F^2	1.036	1.034	1.009	1.027

Table 2
Crystallographic data for compounds **6-9**

	6	**7**	**8**	**9**
Empirical formula	$C_{93}H_{88}Ag_4B_4F_{16}N_6O_3P_4$	$C_{90}H_{85}Ag_4Cl_4F_{12}N_{10}O_{13}P_2S_4$	$C_{102}H_{104}Ag_4F_{12}N_6O_{16}P_4S_4$	$C_{84}H_{72}Ag_2F_6N_6O_6P_4S_2$
Formula mass	2240.29	2506.14	2581.51	1779.22
a (Å)	17.5712(7)	29.5902(15)	9.9341(5)	15.9418(16)
b (Å)	11.3796(4)	12.6772(7)	27.9506(16)	15.4521(14)
c (Å)	23.4529(10)	27.3150(16)	19.8545(12)	16.1046(16)
α (°)	90	90	90	90
β (°)	101.292(2)	108.079(2)	103.234(3)	93.856(3)
γ (°)	90	90	90	90
V (Å^3)	4598.7(3)	9740.6(9)	5366.5(5)	3958.1(7)
Z	2	4	2	2
Crystal system	Monoclinic	Monoclinic	Monoclinic	Monoclinic
Space group	$P2_1/n$	$C2/c$	$P2_1$	$P2_1/c$
T (K)	110(2)	110(2)	110(2)	110(2)
$D_{calc.}$ (g cm^{-3})	1.618	1.709	1.598	1.493
μ (mm^{-1})	0.995	1.110	0.943	0.700
$2\theta_{max}$ (°)	26.53	31.90	26.36	28.36
Reflections measured	88127	16120	48692	49846
Reflections used (R_{int})	9501 (0.0579)	11012 (0.0348)	21138 (0.0431)	9890 (0.0527)
Restraints/parameters	30/614	0/627	344/1266	0/496
R_1 [$I > 2\sigma(I)$]	0.0490	0.0482	0.0475	0.0363
wR_2 [$I > 2\sigma(I)$]	0.1279	0.0983	0.0935	0.0895
$R(F_o^2)$ (all data)	0.0600	0.0822	0.0657	0.0494
$R_w(F_o^2)$ (all data)	0.1355	0.1140	0.1049	0.0975
Goodness-of-fit on F^2	1.054	1.014	1.024	1.047

are in the range of the typical values, with no significant differences in the bond distances or angles.

3.2.2. Crystal and molecular structure of compound **5**

Given the coordinatively unsaturated environment of the silver centers in compound **2** and the labile nature of the Otf$^-$ ion in **3**, design of coordination complexes using additional electron donor ligands appeared to be feasible. Reaction of the bidentate 5,5′-dimethyl-2,2′-bipyridine with a solution containing $AgBF_4$, and the subsequent addition of the PMP-21 gave rise to the formation of compound **5**. Formation of the product is not achieved when

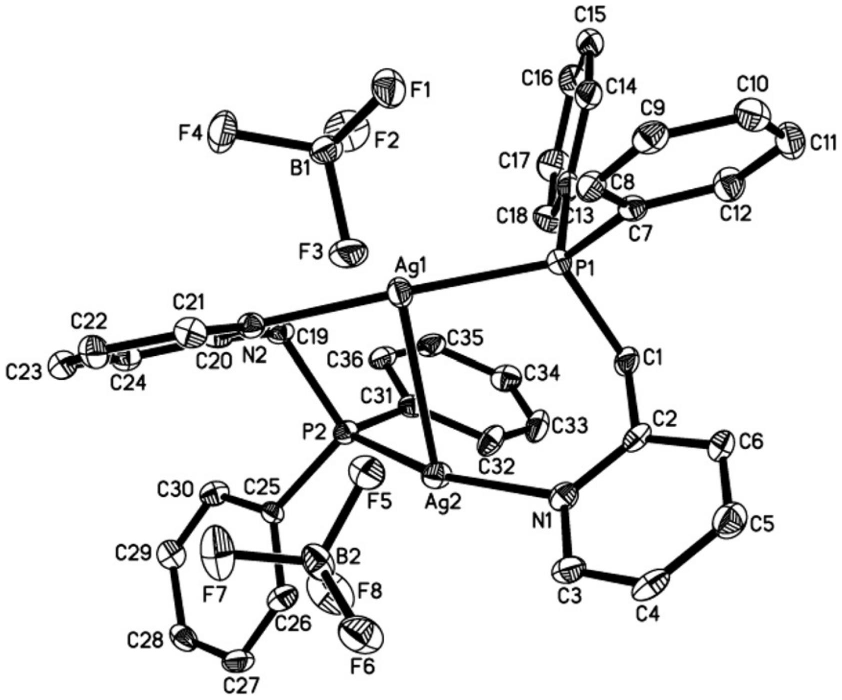

Fig. 2. Thermal ellipsoid plot of **2** with an atomic numbering scheme. Ellipsoids are shown at the 50% level. Hydrogen atoms have been removed for clarity.

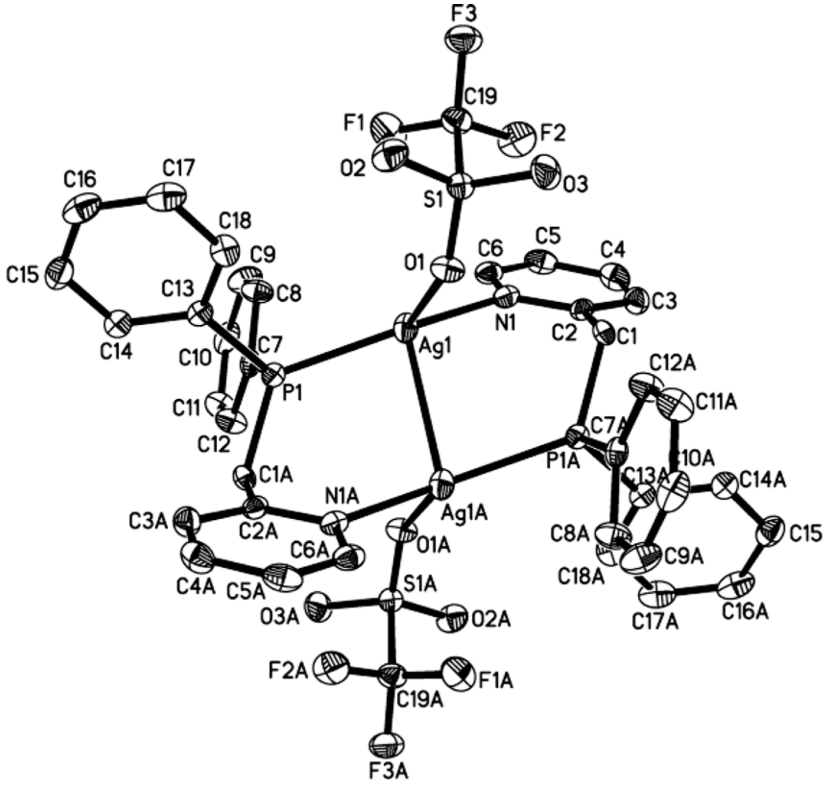

Fig. 3. Thermal ellipsoid plot of **3** with an atomic numbering scheme. Ellipsoids are shown at the 50% level. Hydrogen atoms have been removed for clarity.

the bipyridine ligand is added to a reaction mixture containing the silver salt and the phosphine ligand, which is indicative that in solution the $AgBF_4$:PMP-21 adduct contains a saturated environment that prevents the coordination of another donor ligand. On the other hand, formation of a $AgBF_4$:5,5′-dimethyl-2,2′-bipyridine adduct is

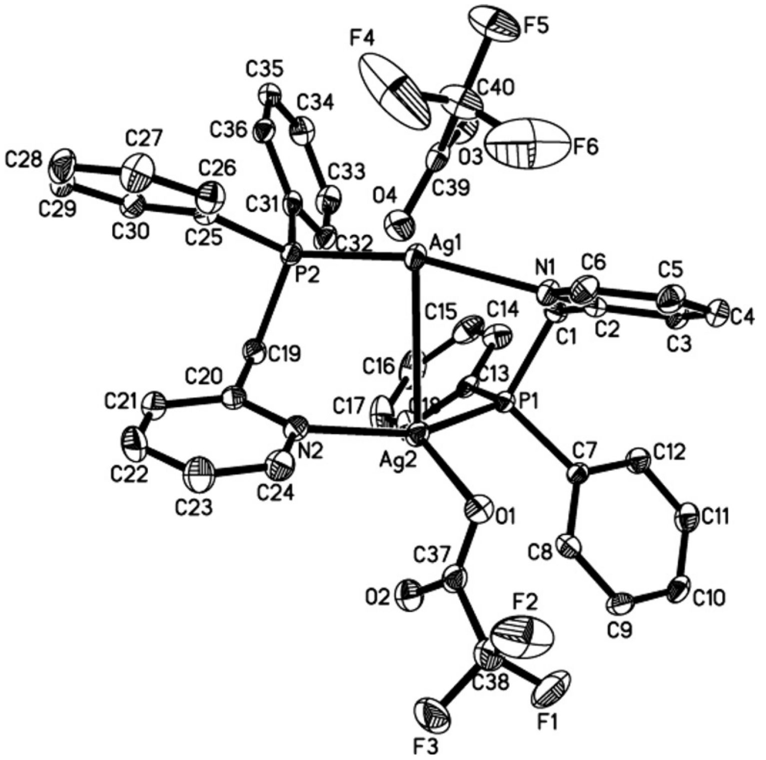

Fig. 4. Thermal ellipsoid plot of **4** with an atomic numbering scheme. Ellipsoids are shown at the 50% level. Hydrogen atoms and two CH_2Cl_2 molecules have been removed for clarity.

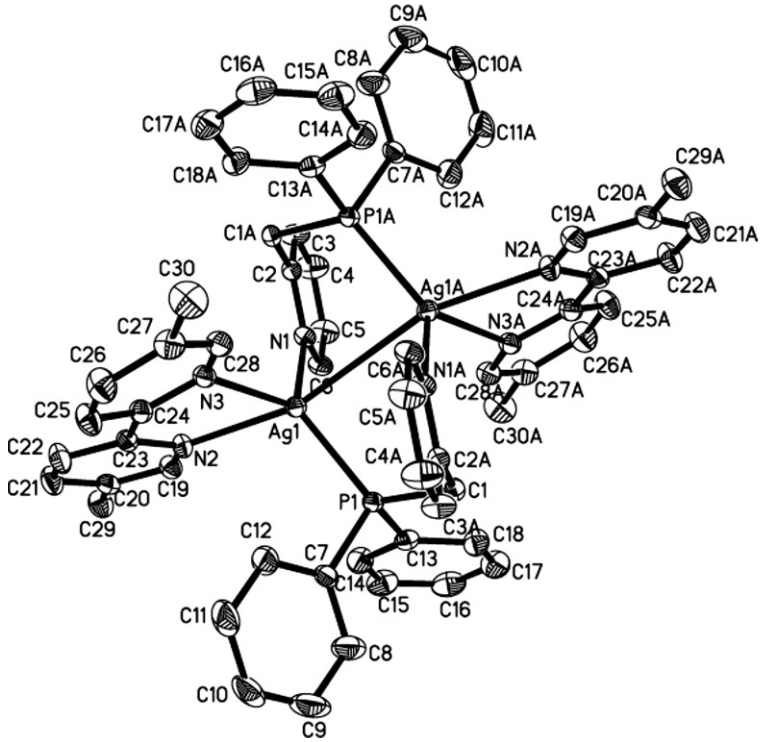

Fig. 5. Thermal ellipsoid plot of the cationic portion of **5** with an atomic numbering scheme. Ellipsoids are shown at the 50% level. Hydrogen atoms have been removed for clarity.

more susceptible to coordination of a P,N-donor ligand. The crystal structure shown in Fig. 5 displays a 1:1:1 ratio of PMP-21 ligand to metal to bipyridine fragment. The expansion of the silver coordination environment from trigonal into a five-coordinate setting was as expected. A distorted trigonal bipyramidal geometry is observed for the

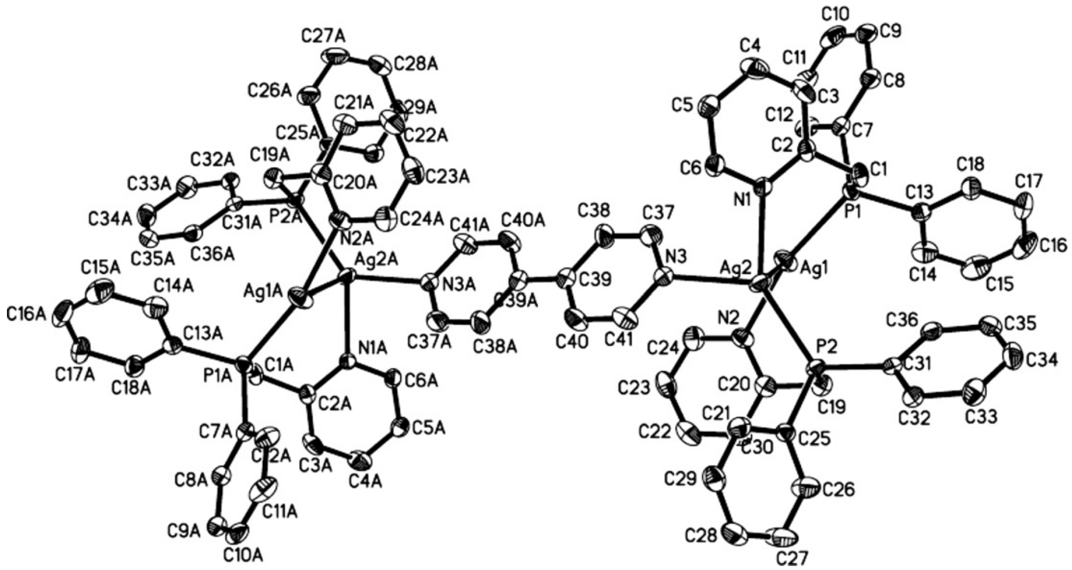

Fig. 6. Thermal ellipsoid plot of the cationic portion of **6** with an atomic numbering scheme. Ellipsoids are shown at the 50% level. Hydrogen atoms and solvent molecules have been removed for clarity.

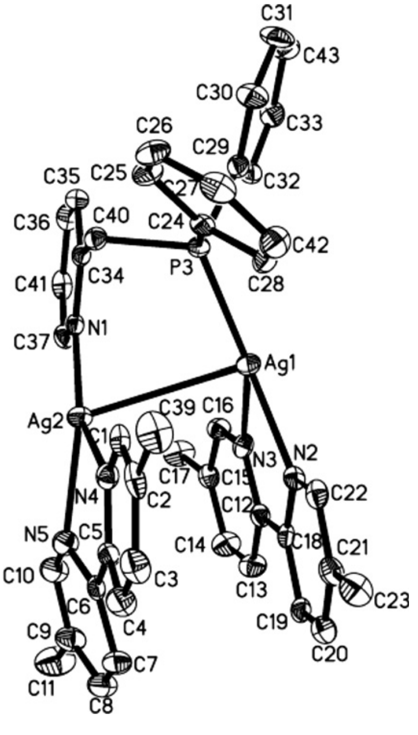

Fig. 7. Thermal ellipsoid plot of the cationic portion of **7** with an atomic numbering scheme. Ellipsoids are shown at the 50% level. Hydrogen atoms and a CH_2Cl_2 molecule have been removed for clarity.

silver ions in compound **5**. The equatorial angles range from 115.6(4)° to 127.5(4)°, where the Ag1–N1, Ag1–N3, and Ag1–P1 bonds conform the equatorial plane, and the axial angle is close to 180° with a value of 163.29(4)° corresponding to the N2–Ag1–Ag1#1 angle. An expected longer Ag–Ag distance is observed (3.2645(5) Å) compared to compound **2**, since electron donation of the bipyridine ligands weakens the metal–metal interaction. The rings of the bipyridine ligand are twisted from planarity at an angle of 17.8(1)°. The center of the Ag–Ag axis lies on a crystallographic inversion center.

3.2.3. Crystal and molecular structure of compound **6**

Using the bifunctional connector, the crystal structure of compound **6** reveals a linked structure supported by the coordination of the 4,4′-bipyridine to two discrete $[AgBF_4(PMP\text{-}21)]_2$ molecules. 4,4′-Bipyridine is an ideal connector between metal atoms for the prolongation of coordination networks, due to two binding sites which are arranged in a divergent (exo) fashion. It also has a rigid structure which will help in the predictability of the network geometries, and the length of the ligand is appropriate to create cavities of molecular dimensions upon the formation of the networks with metal atoms [35]. Compound **6** shown in Fig. 6 is obtained by addition of 1/2 equiv. of 4,4′-bipyridine to a reaction mixture containing a 1:1 ratio of PMP-21 ligand to $AgBF_4$. Ag1 has a slightly distorted T-shaped geometry, confirmed by the approximately perpendicular angles of 90.8(3)° and 82.6(1)° and the closely linear conformation in N2–Ag1–P1 with a value of 164.4(1)°. The coordination sphere of Ag2 displays a distorted tetrahedral conformation due to the coordination of the bipyridine ligand, with angles ranging between 84.2(1)° and 122.3(1)°. The Ag–Ag interaction in the typical lengths at 2.9989(5) Å, is rather less affected by the presence of the 4,4′-bipyridine ligand compared with the silver interaction in compound **5**. The conformation of the phosphine ligand in compound **6** is analogous to compound **5**, displaying torsion angles with values of 78.4(4)° for P1–C1–C2–N1 and 79.2(4)° for P2–C19–C20–N2. The middle of the bipy connecting ligand lies on a crystallographic inversion center.

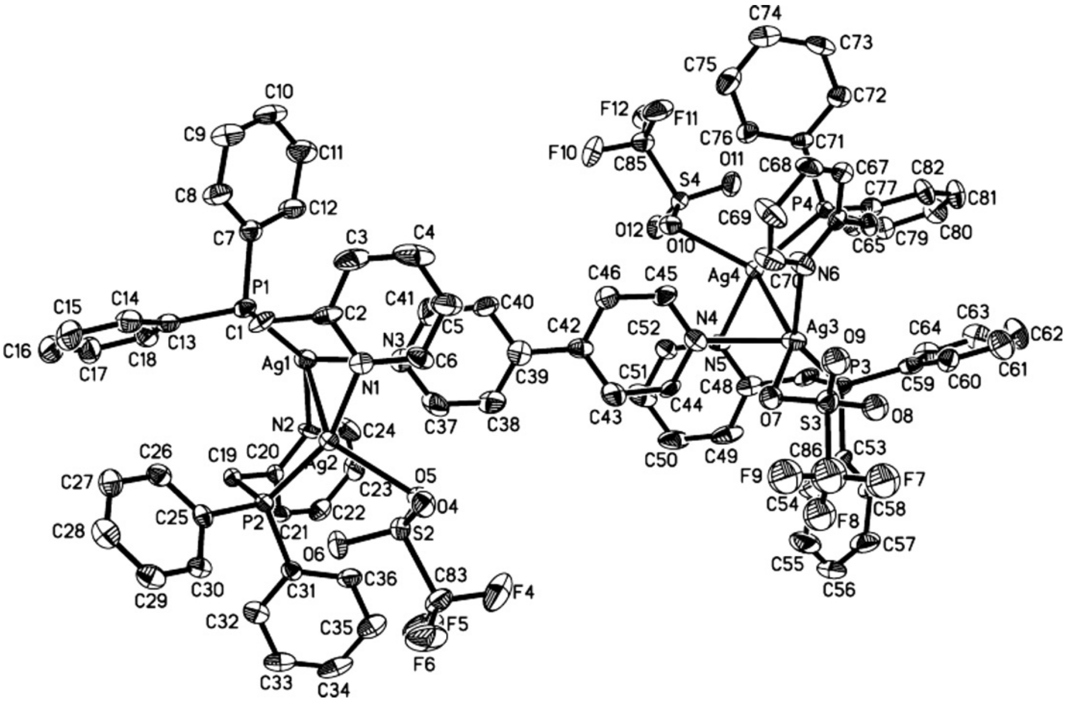

Fig. 8. Thermal ellipsoid plot of **8** with an atomic numbering scheme. Ellipsoids are shown at the 50% level. Hydrogen atoms have been removed for clarity.

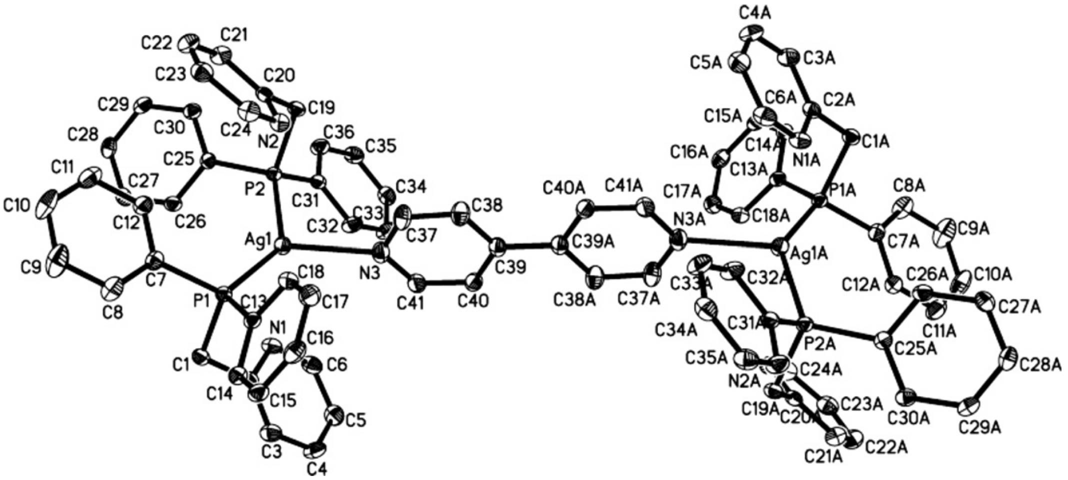

Fig. 9. Thermal ellipsoid plot of the cationic portion of **9** with an atomic numbering scheme. Ellipsoids are shown at the 50% level. Hydrogen atoms have been removed for clarity.

3.2.4. Crystal and molecular structure of compound 7

Compound **7** presents a different ligand/metal ratio where there are one PMP-21 ligands, two silvers and two 5,5′-dimethyl-2,2′-bipyridines as shown in Fig. 7. With the shortest Ag–O distance being 4.5894(3) Å (Ag2–O1) there is no interaction of the Ag centers with the anions. The cationic portion of **7** does however have π–π interactions from adjacent molecules which results in the formation of a chain of cations down the crystallographic *b*-axis. The pyridyl rings of the bipyridine ligand bound to Ag1 which is P-bound by the PMP-21 remains nearly coplanar, evidenced by the small angle of 6.18(5)°, while the other bipyridine connected to Ag2, which is N-bound by the PMP-21 displays a larger twisting angle of 18.2(8)°. Angles around the silver ions indicate a capped trigonal planar geometry, ranging from 73.2(1)° to 141.9(9)° for Ag1 and 73.4(1)° to 153.4(1)° for Ag2.

3.2.5. Crystal and molecular structure of compounds 8 and 9

Compounds **8** and **9** show the result of the reaction of the PMP-21 ligand with AgOtf in a 1:1 and 2:1 ratio respectively, with subsequent addition of 1/2 equiv. of 4,4′-bipyridine. The crystal structure of compound **8** is analogous to compound **6** where two [AgOtf(PMP-21)]$_2$ units are linked

Table 3
Selected bond lengths (Å), angles (°), and distances for the compounds [AgBF$_4$(PMP-21)]$_2$ (**2**), [AgOtf(PMP-21)]$_2$ (**3**), and [Agtfa(PMP-21)]$_2$ (**4**)[a]

2			
Ag(1)–Ag(2)	2.9219(4)	Ag(2)–P(2)	2.3649(10)
Ag(1)–P(1)	2.3752(11)	Ag(2)–N(1)	2.187(3)
Ag(1)–N(2)	2.198(3)		
N(2)–Ag(1)–P(1)	163.2(8)	N(1)–Ag(2)–P(2)	160.4(8)
N(2)–Ag(1)–Ag(2)	86.8(7)	N(1)–Ag(2)–Ag(1)	92.2(8)
P(1)–Ag(1)–Ag(2)	86.0(3)	P(2)–Ag(2)–Ag(1)	87.9(3)
3			
Ag(1)–Ag(1)#1	2.7979(10)	Ag(1)–P(1)	2.3860(15)
Ag(1)–N(1)	2.201(4)	Ag(1)–O(1)	2.456(3)
N(1)–Ag(1)–P(1)	144.0(1)	N(1)–Ag(1)–Ag(1)#1	103.4(1)
N(1)–Ag(1)–O(1)	100.3(1)	P(1)–Ag(1)–Ag(1)#1	84.50(4)
P(1)–Ag(1)–O(1)	114.8(9)	O(1)–Ag(1)–Ag(1)#1	91.17(8)
4			
Ag(1)–Ag(2)	3.0538(4)	Ag(1)–P(2)	2.4010(9)
Ag(2)–P(1)	2.3796(9)	Ag(1)–N(1)	2.282(3)
Ag(2)–N(2)	2.253(3)	Ag(2)–O(1)	2.449(2)
N(1)–Ag(1)–P(2)	155.2(7)	P(1)–Ag(2)–O(1)	114.7(6)
N(1)–Ag(1)–Ag(2)	76.1(7)	N(2)–Ag(2)–Ag(1)	80.1(7)
P(2)–Ag(1)–Ag(2)	86.5(2)	P(1)–Ag(2)–Ag(1)	88.5(2)
N(2)–Ag(2)–P(1)	153.2(8)	O(1)–Ag(2)–Ag(1)	105.9(6)
N(2)–Ag(2)–O(1)	91.9(9)		

[a] Symmetry transformations used to generate equivalent atoms. For **3**: #1 = $-x + 1, -y + 1, -z + 1$.

Table 4
Selected bond lengths (Å), angles (°), and distances for the compounds [AgBF$_4$(PMP-21)(5,5′-dimethyl-2,2′-bipyridine)]$_2$ (**5**) and [AgBF$_4$(PMP-21)]$_4$(4,4′-bipyridine) (**6**)[a]

5			
Ag(1)–Ag(1)#1	3.2645(5)	Ag(1)–P(1)	2.3808(6)
Ag(1)–N(1)	2.2995(16)	Ag(1)–N(2)	2.4211(17)
Ag(1)–N(3)	2.3979(16)		
N(1)–Ag(1)–P(1)	127.50(4)	N(1)–Ag(1)–N(3)	116.53(6)
P(1)–Ag(1)–N(3)	115.54(4)	N(1)–Ag(1)–N(2)	91.57(6)
P(1)–Ag(1)–N(2)	112.79(4)	N(2)–Ag(1)–Ag(1)#1	163.29(4)
6			
Ag(1)–Ag(2)	2.9989(5)	Ag(1)–P(1)	2.3624(11)
Ag(2)–P(2)	2.3623(11)	Ag(1)–N(2)	2.172(4)
Ag(2)–N(1)	2.254(4)		
N(2)–Ag(1)–P(1)	164.43(10)	N(2)–Ag(1)–Ag(2)	82.58(10)
P(1)–Ag(1)–Ag(2)	90.78(3)	N(1)–Ag(2)–P(2)	145.44(9)
N(1)–Ag(2)–N(3)	91.36(13)	P(2)–Ag(2)–N(3)	122.25(10)
N(1)–Ag(2)–Ag(1)	91.21(9)	P(2)–Ag(2)–Ag(1)	85.08(3)
N(3)–Ag(2)–Ag(1)	84.20(10)		

[a] Symmetry transformations used to generate equivalent atoms. For **5**: #1 = $-x + 1, -y, -z + 2$.

together by coordination of the 4,4′-bipyridine. The molecular structure of compound **8**, displayed in Fig. 8, shows different coordination geometries for the different silver atoms. Ag1 has a distorted tetrahedral geometry where the previously binding triflate from **3** has been replaced by the 4,4′-bipyridine. Ag2 which is coordinated with a Otf anion presents a distorted tetrahedral geometry with angles varying between 84.6(2)° and 159.2(2)°. Ag3 has a distorted trigonal bipyramidal geometry, where the axis is formed by the interaction of Ag3 with Ag4 and O7. In Ag4 a highly distorted tetrahedral geometry is encountered with angles ranging between 84.6(2)° and 157.2(2)°. The X-ray crystal structure of compound **8** also has four THF molecules, two of which are disordered, and one unbound Otf anion. The Otf anion bound to Ag3 is disordered such that only 54% of the time it is actually bound to the silver, the other 46% of the time it is slightly further away and outside bonding distance. The Ag–Ag interactions are seen

Table 5
Selected bond lengths (Å), angles (°), and distances for the compounds $(AgOtf)_2(PMP\text{-}21)(5,5'\text{-dimethyl-}2,2'\text{-dipyridyl})_2$ (**7**) $[AgOtf(PMP\text{-}21)]_4(4,4'\text{-bipyridine})$ (**8**), and $[AgOtf(PMP\text{-}21)_2]_2(4,4'\text{-bipyridine})$ (**9**)

7			
Ag(1)–Ag(2)	3.1430(5)	Ag(1)–P(3)	2.3402(10)
Ag(2)–N(1)	2.155(3)	Ag(1)–N(2)	2.301(3)
Ag(1)–N(3)	2.280(4)	Ag(2)–N(4)	2.245(3)
Ag(2)–N(5)	2.328(3)	Ag(2)–O(1)	4.589(3)
N(3)–Ag(1)–N(2)	73.2(1)	N(3)–Ag(1)–P(3)	141.9(9)
N(2)–Ag(1)–P(3)	141.9(1)	N(3)–Ag(1)–Ag(2)	73.5(9)
N(2)–Ag(1)–Ag(2)	95.2(9)	P(3)–Ag(1)–Ag(2)	86.1(3)
N(1)–Ag(2)–N(4)	153.4(1)	N(1)–Ag(2)–N(5)	132.8(1)
N(4)–Ag(2)–N(5)	73.4(1)	N(1)–Ag(2)–Ag(1)	83.3(9)
N(4)–Ag(2)–Ag(1)	79.7(9)	N(5)–Ag(2)–Ag(1)	114.7(1)
8			
Ag(1)–Ag(2)	3.0816(8)	Ag(3)–Ag(4)	3.0538(9)
Ag(1)–P(1)	2.375(2)	Ag(2)–P(2)	2.3642(19)
Ag(3)–P(3)	2.3633(19)	Ag(4)–P(4)	2.3730(19)
Ag(1)–N(2)	2.283(6)	Ag(1)–N(3)	2.341(7)
Ag(2)–N(1)	2.191(7)	Ag(3)–N(4)	2.367(6)
Ag(3)–N(6)	2.285(7)	Ag(4)–N(5)	2.216(6)
N(2)–Ag(1)–N(3)	92.2(2)	N(2)–Ag(1)–P(1)	143.7(2)
N(3)–Ag(1)–P(1)	120.8(2)	N(2)–Ag(1)–Ag(2)	89.3(2)
N(3)–Ag(1)–Ag(2)	73.3(2)	P(1)–Ag(1)–Ag(2)	86.52(5)
N(1)–Ag(2)–P(2)	159.2(2)	N(1)–Ag(2)–O(5)	88.9(2)
P(2)–Ag(2)–O(5)	110.4(1)	N(1)–Ag(2)–Ag(1)	84.6(2)
P(2)–Ag(2)–Ag(1)	86.5(5)	O(5)–Ag(2)–Ag(1)	135.9(1)
N(6)–Ag(3)–P(3)	140.8(2)	N(6)–Ag(3)–N(4)	92.2(2)
P(3)–Ag(3)–N(4)	123.1(2)	O(7A)–Ag(3)–Ag(4)	148.6(2)
N(5)–Ag(4)–P(4)	157.2(2)	N(5)–Ag(4)–O(10)	86.4(2)
P(4)–Ag(4)–O(10)	114.3(1)	N(5)–Ag(4)–Ag(3)	84.6(2)
P(4)–Ag(4)–Ag(3)	85.7(5)	O(10)–Ag(4)–Ag(3)	138.3(1)
9			
Ag(1)–P(1)	2.4384(6)	Ag(1)–P(2)	2.4274(6)
Ag(1)–N(3)	2.3924(19)		
N(3)–Ag(1)–P(2)	105.2(5)	N(3)–Ag(1)–P(1)	112.7(5)
P(2)–Ag(1)–P(1)	139.1(2)		

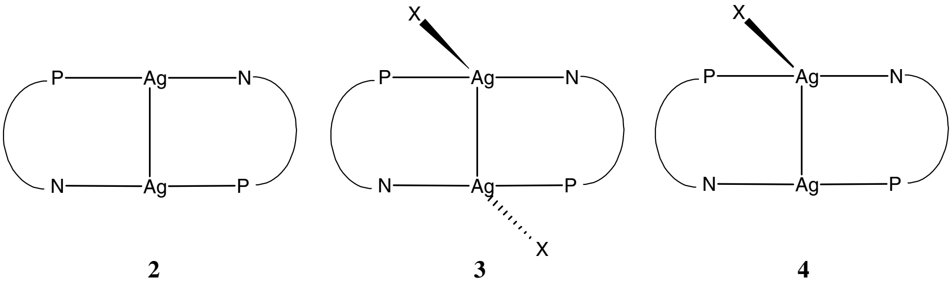

Scheme 1.

to be weakened by the coordination of the bipyridine ligand, compared to the metallophilic interactions encountered in compound **3**. All Ag–P and Ag–N distances fall in the range of reported values.

Compound **9** is representative of an intermediate structural compound when moving from the 1:1 to 2:1 ratios of PMP-21 ligand to metal. The PMP-21 ligands are monodentate as shown in Fig. 9, with the Ag1 atom too far removed from the N1 and N2 atoms (2.6575(2) and 3.2591(2) Å, respectively) to describe any strong interaction. The angles around the metal center indicate a distorted trigonal planar geometry, with angles ranging between 105.18(5)° and 139.08(2)°. The center of the bipyridine ligands sits on a crystallographic inversion center. Attempts to prepare the analogous compound with triphenylphosphine in place of the PMP-21 ligand resulted only in the crystallization of $AgOtf(PPh_3)_4$ as the main product of the reaction. This leads to the conclusion that not only steric, but also electronic factors provided by the pyridyl group contribute to the formation of compound **9**.

3.3. Luminescence properties

Coordination complexes that present luminescent properties have attracted increasing attention because of their potential applications as light-emitting devices, in areas of optoelectronic devices and chemical sensors [36–38]. Organic compounds with aromatic nitrogen heterocycles, which can be receptors for metal ions, have been studied extensively because they are capable of performing useful light- and/or redox-induced tasks [39–41]. Particularly, luminescence complexes of some transition metals of the group VII and VIII containing bipyridine type ligands have attracted much attention because of their high luminescent efficiency [42–45]. However, the low yields and higher costs of these complexes are disadvantages for their use as optoelectronic materials. The lower cost of d^{10} metal complexes with nitrogen and phosphorous containing ligands are of interest because of their photoluminescent properties [42–46]. Here, we report the excitation and emission spectra of the metal complexes, all spectra were recorded at concentrations of 1×10^{-4} M in acetonitrile glasses at 77 K. In solution at room temperature there is no observable fluorescence.

The similarity of the excitation spectra of compounds **2**–**4** is not surprising, given the same structural conformation of the phosphine ligand with the silver metal in the complexes, which is the result of a ligand-to-metal charge transfer. Excitation maxima for **2**, **3**, and **4** are 300, 297, and 295 nm, respectively. The emission spectra show a single maximum for each case, illustrating the decay transitions associated with each system. Excitation maxima of all compounds are presented in Table 6 along with the local emission maxima. The emission spectra of all the compounds cover a wide range of the spectrum with local maxima spanning approximately 200 nm, showing in the case of the bipyridine substituted complexes multiple maxima, illustrating the complexity of the decay transitions associated with the more complicated system. Comparing the emission data of the series of compounds obtained with the $AgBF_4$ salt, a red shift of the maximum of approximately 100 nm is observed for the $[AgBF_4(PMP\text{-}21)]_2$ complex with respect to any of the species coordinated either with the 5,5′-dimethyl-2,2′-bipyridine or 4,4′-bipyridine. Also the emission spectrum of complex **2** is noticeably more intense than **5** and **6**. The same luminescent behavior is observed for the series of compounds synthesized with the AgOtf salt, where the maximum in the emission spectrum of the $[AgOtf(PMP\text{-}21)]_2$ compound is red shifted with respect to compounds **7**, **8**, and **9**. A stronger shift occurs between **3** and **7** in the presence of the 5,5′-dimethyl-2,2′-bipyridine. Comparing the emission spectra of compounds **8** and **9**, which differ in the coordination of two PMP-21 ligands to the silver atom in **9** and only one through the phosphorus atom in compound **8**, no major differences in maxima location and intensity is observed. The excitation maxima of the compounds substituted with a bipyridine ligand cover a short range of wavelengths between 291 and 323 nm. As described also for the emission spectra, compounds **5** and **7** exhibit the largest excitation maxima shift to the red compared to the corresponding $[AgBF_4(PMP\text{-}21)]_2$ and $[AgOtf(PMP\text{-}21)]_2$ complexes.

Table 6
Luminescent spectral data for compounds **2**–**9** at 77 K and 1×10^{-4} M in CH_3CN

Compound	Excitation, λ_{max} (nm)	Emission local, λ_{min} (nm)
2	300	392, 402
3	297	389
4	295	392
5	323	455, 483, 507
6	313	438, 468, 493
7	329	451, 483
8	291	410, 435
9	299	411, 438

4. Conclusions

We have demonstrated in this study the ability of the PMP-21 ligand to act as a bridging bidentate ligand for the formation of Ag coordination complexes containing a Ag–Ag argentophilic interaction. Structures formed with BF_4^-, Otf^-, or tfa^- as the counterion show little structural dependence on the interaction of the anion when reacted in a 1:1 ratio. For both the BF_4^- and Otf^- derivatives, additional reactivity at the silver center has been demonstrated by the formation of complexes containing 5,5′-dimethyl-2,2′-bipyridine or 4,4′-bipyridine. Which result in highly in crowded metal centers for the 5,5′-dimethyl-2,2′-bipyridine derivatives and linked dimers for the 4,4′-bipyridine derivatives. A unique structure containing a bridging 4,4′-bipyridine has been found when the ratio of PMP-21 to silver is 2:1. As expected, all of the compounds reported exhibit luminescence at 77 K.

Work continues on the synthesis and coordination chemistry of interesting pyridyl-containing phosphines. A new ligand PMP-41, where the pyridine is substituted in the 4-position, has been synthesized and its coordination behavior with silver salts studied. The chemistry of the PMP-21 ligand has also been extended to the doubly substituted phenylphosphino-bis-2-methylpyridine (PMP-22) which can act as a chelate and a pincer ligand at the same time. Manuscripts concerning the results of the coordination chemistry of these ligands are currently in preparation.

Acknowledgements

This research was supported by funds provided by grant from the Robert A. Welch Foundation (AA-1508). The Bruker X8 APEX diffractometer was purchased with funds received from the national Science Foundation Major Research Instrumentation Program Grant CHE-0321214. Baylor University's Varian 500 MHz NMR was funded by the National Science Foundation's Major Research Instrumentation program, Award # CHE-0420802.

Appendix A. Supplementary data

CCDC 648315, 648316, 648317, 648318, 648319, 648320, 648321 and 648322 for **2**, **3**, **4**, **5**, **6**, **7**, **8** and **9**. These data can be obtained free of charge via http://www.ccdc.cam.ac.uk/conts/retrieving.html, or from the Cambridge Crystallographic Data Centre, 12 Union Road, Cambridge CB2 1EZ, UK; fax: (+44) 1223-336-033; or e-mail: deposit@ccdc.cam.ac.uk. Supplementary data associated with this article can be found, in the online version, at doi:10.1016/j.ica.2007.08.015.

References

[1] G.R. Newkome, Chem. Rev. 93 (1993) 2067.
[2] Z.Z. Zhang, H. Cheng, Coord. Chem. Rev. 147 (1996) 1.
[3] P. Espinet, K. Soulantica, Coord. Chem. Rev. 193 (1999) 499.
[4] A. Cingolani, E. Di Nicola, D. Martini, C. Pettinari, B.W. Skelton, A.H. White, Inorg. Chim. Acta 359 (2006) 2183.
[5] A. Murso, M. Straka, M. Kaupp, R. Bertermann, D. Stalke, Organometallics 24 (2005) 3576.
[6] B. Åkermark, B. Krakenberger, S. Hansson, A. Vitagliano, Organometallics 6 (1987) 620.
[7] W.J. Knebel, R.J. Angelici, Inorg. Chem. 13 (1974) 632.
[8] W.J. Knebel, R.J. Angelici, Inorg. Chim. Acta 7 (1973) 713.
[9] P. Braunstein, B.T. Heaton, C. Jacob, L. Manzi, X. Morise, Dalton Trans. (2003) 1396.
[10] M. Jansen, Angew. Chem., Int. Ed. Engl. 26 (1987) 1098.
[11] P. Pyykkö, Chem. Rev. 97 (1997) 597.
[12] P. Pyykkö, Angew. Chem., Int. Ed. Engl. 43 (2004) 4412.
[13] C. Janiak, Dalton Trans. (2000) 3885.
[14] C.M. Che, Z. Mao, V.M. Miskowski, M.C. Tse, C.K. Chan, K.K. Cheung, D.L. Phillips, K. Hung, Angew. Chem., Int. Ed. Engl. 39 (2000) 4084.
[15] R.P. Feazell, C.E. Carson, K.K. Klausmeyer, Eur. J. Inorg. Chem. (2005) 3287.
[16] R.P. Feazell, C.E. Carson, K.K. Klausmeyer, Inorg. Chem. 45 (2006) 935.
[17] R.P. Feazell, C.E. Carson, K.K. Klausmeyer, Inorg. Chem. 45 (2006) 2627.
[18] R.P. Feazell, C.E. Carson, K.K. Klausmeyer, Inorg. Chem. 45 (2006) 2635.
[19] S.R. Batten, R. Robson, Angew. Chem., Int. Ed. Engl. 37 (1998) 1460.
[20] D. Venkataraman, G.B. Gardner, S. Lee, J.S. Moore, J. Am. Chem. Soc. 117 (1995) 11600.
[21] D.M. Goodgame, D.A. Garchvogel, D.J. Williams, Angew. Chem., Int. Ed. Engl. 38 (1999) 153.
[22] S. Kitagawa, R. Kitaura, S. Noro, Angew. Chem., Int. Ed. Engl. 43 (2004) 2334.
[23] S. Kitagawa, S. Noro, R. Nakamura, Chem. Commun. (2006) 701.
[24] K.K. Klausmeyer, R.P. Feazell, J.H. Reibenspies, Inorg. Chem. 43 (2004) 1130.
[25] R.P. Feazell, C.E. Carson, K.K. Klausmeyer, Inorg. Chem. 44 (2005) 996.
[26] C. Di Nicola, Effendy, F. Marchetti, C. Pettinari, B.W. Skelton, A.H. White, Inorg. Chim. Acta 360 (2007) 1433.
[27] Effendy, F. Marchetti, C. Pettinari, B.W. Skelton, A.H. White, Inorg. Chim. Acta 360 (2007) 1424.
[28] Effendy, F. Marchetti, C. Pettinari, R. Pettinari, B.W. Skelton, A.H. White, Inorg. Chim. Acta 360 (2007) 1414.
[29] Effendy, F. Marchetti, C. Pettinari, R. Pettinari, B.W. Skelton, A.H. White, Inorg. Chim. Acta 360 (2007) 1451.
[30] M.O. Awaleh, A. Badia, F. Brisse, Cryst. Growth Des. 6 (2006) 2674.
[31] I. Moldes, E. de la Encarnacion, J. Rosa, A. Alvarez-Larena, J.F.J. Piniella, Organomet. Chem. 566 (1998) 156.
[32] E. de la Encarnacion, J. Pons, R. Yanez, J. Roz, Inorg. Chim. Acta 359 (2006) 745.
[33] H. Brunner, C. Valerio, M. Zabel, New J. Chem. 24 (2000) 275.
[34] X.B. Jiang, L. Lefort, P.E. Goudriaan, A.H.M. de Vries, P.W. van Leeuwen, J.G. de Vries, J.N. Reek, Angew. Chem. Int. Ed. Engl. 45 (2006) 1223.
[35] K. Biradha, M. Sarkar, L. Rajput, Chem. Commun. (2006) 4169.
[36] A. Bacher, C.H. Erdelen, W. Paulus, H. Ringsdorf, H. Schmidt, P. Schuhmacher, Macromolecules 32 (1999) 4551.
[37] S.N. Wang, Coord. Chem. Rev. 215 (2001) 79.
[38] C.H. Chen, J. Shi, Coord. Chem. Rev. 171 (1998) 161.
[39] Q.G. Wu, J.A. Lavigne, Y. Tao, M. D'Lorio, S.N. Wang, Inorg. Chem. 39 (2000) 5428.
[40] Q.G. Wu, A. Hook, S.N. Wang, Angew. Chem., Int. Ed. Engl. 39 (2000) 3933.
[41] D.T. Song, S.N. Wang, Eur. J. Inorg. Chem. (2003) 3774.
[42] M.L. Tong, X.M. Chen, B.H. Ye, L.N. Ji, Angew. Chem., Int. Ed. Engl. 38 (1999) 2237.
[43] X.M. Zhang, M.L. Tong, M.L. Gong, H.K. Lee, L. Luo, K.F. Li, Y.X. Tong, X.M. Chen, Chem. Eur. J. 8 (2002) 3187.
[44] G. Yu, S.W. Yin, Y.Q. Liu, A.G. Shuai, D.B. Zhu, J. Am. Chem. Soc. 125 (2003) 14816.
[45] W.K. Lo, W.K. Wong, W.Y. Wong, J.P. Guo, Eur. J. Inorg. Chem. (2005) 3950.
[46] R.Q. Fan, D.S. Zhu, Y. Mu, G.H. Li, Y.L. Yang, Q. Su, Eur. J. Inorg. Chem. (2004) 4891.